European Journal of Pharmaceutics and Biopharmaceutics 74 (2010) 55–66

Contents lists available at ScienceDirect

European Journal of Pharmaceutics and Biopharmaceutics

journal homepage: www.elsevier.com/locate/ejpb

Research paper

Application of Electron Paramagnetic Resonance (EPR) spectroscopy and imaging in drug delivery research – Chances and challenges

Sabine Kempe, Hendrik Metz, Karsten Mäder *

Martin-Luther-University Halle-Wittenberg, Department of Pharmaceutics and Biopharmaceutics, Halle/Saale, Germany

ARTICLE INFO

Article history:
Received 12 March 2009
Accepted in revised form 25 August 2009
Available online 31 August 2009

Keywords:
EPR
ESR
Electron Spin Resonance
Electron Paramagnetic Resonance
Drug delivery
EPR imaging
In vivo

ABSTRACT

Electron Paramagnetic Resonance (EPR) spectroscopy is a powerful technique to study chemical species with unpaired electrons. Since its discovery in 1944, it has been widely used in a number of research fields such as physics, chemistry, biology and material and food science. This review is focused on its application in drug delivery research. EPR permits the direct measurement of microviscosity and micropolarity inside drug delivery systems (DDS), the detection of microacidity, phase transitions and the characterization of colloidal drug carriers. Additional information about the spatial distribution can be obtained by EPR imaging. The chances and also the challenges of *in vitro* and *in vivo* EPR spectroscopy and imaging in the field of drug delivery are discussed.

1. Introduction

Electron Paramagnetic Resonance (EPR), also known as Electron Spin Resonance (ESR), is a spectroscopy technique that allows the direct and non-invasive detection of paramagnetic species consisting of one or more unpaired electrons in complex and non-transparent samples. This species include short living or stable free radicals (e.g. spin probes, Fig. 1) or transition metal ions, such as Mn^{2+}, Fe^{3+} and Cu^{2+}. Since its discovery by Zavoiskii in 1944 [1], EPR has been widely used in a number of research fields such as physics, chemistry, biology and material and food science. Several textbooks have been published explaining the elementary theory and application of EPR in these fields [2–4]. The aim of the present review is to give an overview on the different applications of EPR in the field of drug delivery research. Therefore, several representative examples will be presented to show the principal suitability of EPR spectroscopy and imaging, not covering all pharmaceutical applications. Instead, we would like to show not only the potential but also the limitations of these technologies.

The basic principles of EPR are very similar to the more familiar nuclear magnetic resonance (NMR). Both methods are based on the interaction of electromagnetic radiation with magnetic moments caused by electrons (EPR) or nuclei (NMR). The magnetic moment of an unpaired electron arises from its "spin" and when placed in an external magnetic field; the electron spin will align parallel or antiparallel in the direction of the magnetic field, which corresponds to a lower ($M_s = -½$) or an upper ($M_s = +½$) energy state. The energy difference (ΔE) between these two states is proportional to the strength of the applied magnetic field (B_0):

$$\Delta E = h\nu = g\mu_B B_0,$$

where h is Planck's constant, ν is the frequency of the electromagnetic radiation, g is a constant termed g factor ($g = 2.0023$ for an unpaired electron), and μ_B is the Bohr magneton.

If electromagnetic radiation corresponding to the energy difference is applied to the sample, resonance transition is possible between the lower and the upper energy states [2,5]. The EPR resonance frequency is 10^3 times higher compared to NMR frequencies due to the larger magnetic moment of the electron, and this explains the greater sensitivity of EPR with respect to NMR. Free radical concentrations as low as 0.5–1 nmol/ml are EPR detectable [6]. However, the detection limit depends strongly on the line width of the EPR signal, and so differences of several orders of magnitude might be possible (e.g. for the detection of metal ions).

Due to the interaction of the unpaired electron with neighbouring nuclear spins in the MHz range, the splittings are 10^6 times higher compared to NMR. Furthermore, EPR relaxation times are about 10^6 times shorter (ns range) than in NMR, which makes

* Corresponding author. Martin-Luther-University Halle-Wittenberg, Institute of Pharmacy, Department of Pharmaceutics and Biopharmaceutics, Wolfgang-Langenbeck-Str. 4, 06120 Halle/Saale, Germany. Tel.: +49 345 5525167; fax: +49 345 5527029.
E-mail addresses: karsten.maeder@pharmazie.uni-halle.de, maeder@pharmazie.uni-halle.de (K. Mäder).

0939-6411/$ - see front matter © 2009 Elsevier B.V. All rights reserved.
doi:10.1016/j.ejpb.2009.08.007

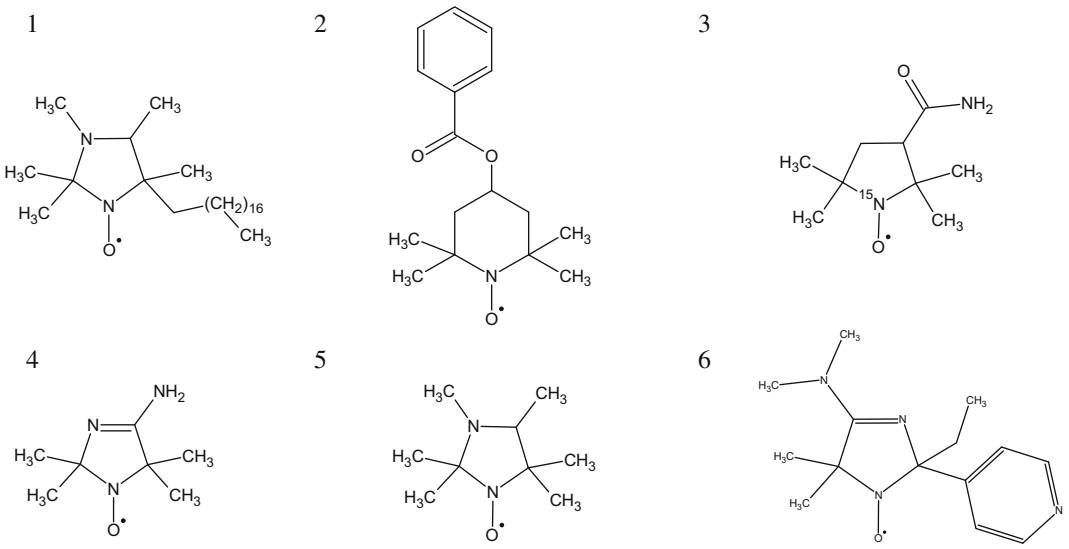

Fig. 1. Examples of spin probes with different physicochemical properties (1 and 2) lipophilic spin probes, (3) hydrophilic spin probes, (4–6) pH-sensitive spin probes. Nomenclature: (1) HD-PMI – 2-Heptadecyl-2,3,4,5,5-pentamethyl-imidazoline-1-oxyl. (2) TB (Tempolbenzoate) – 4-Benzoyloxy-2,2,6,6-tetramethylpiperidine-1-oxyl. (3) ^{15}N-PCM – 3-Carbamoyl-2,2,5,5-tetramethyl-3-pyrrolidin-1-oxyl-1^{15}N. (4) AT (ATI) – 4-Amino-2,2,5,5-tetramethyl-3-imidadoline-1-oxyl. (5) HM – 2,2,3,4,5,5-Hexamethyl-imidazoline-1-oxyl. (6) 2PK – 4-Dimethylamino-5,5-dimethyl-2ethyl-2-pyridin-4-yl-2,5-dihydro-1H-imidazol-1-oxyl.

the implementation of pulsed techniques much more difficult in a practical sense.

Commonly used EPR frequencies in drug delivery research are in the microwave range at 10 GHz (X-band) or 1 GHz (L-band). The L-band spectrometers are not as sensitive as X-band spectrometers, but they have the advantage of the higher penetrating depth of the irradiation of about 5–10 mm into water-containing samples, allowing the measurement of hydrated pellets and tablets or small animals such as mice. For X-band experiments, the microwave penetration depth is limited to 0.5–1 mm in water-rich samples due to the high dielectric constant and the microwave absorption of water or other high polar liquids. Therefore, high frequency EPR is very size limited on water-containing biological and pharmaceutical samples. However, suspensions of micro- or nanoparticles, emulsions and also isolated skin can be measured at 10 GHz in capillaries, flat or tissue cells.

The unpaired electron may interact with neighbouring magnetic nuclei to produce splittings in the EPR spectrum, called hyperfine splittings. The type and number of the nuclei interacting with the electron determine the number of lines and their relative intensities. Therefore, magnetic interaction between the free electron and the nuclear spin of nitrogen (I = 1, ^{14}N) in, for example, nitroxyl radicals results in a hyperfine splitting into three lines (Fig. 2). In contrast, the EPR spectrum of the ^{15}N spin probes shows only two lines because of the interaction of the unpaired electron with the different nuclear spin of the ^{15}N nuclei (I = ½). The unpaired electron is only partially localized in the p_z-orbital of the nitrogen atom. It can be also localized at the oxygen atom or delocalized over the ring structure of these nitroxyl radicals. Therefore, nitroxyl radicals are very sensitive to small charge density variations caused by surrounding molecules. The strength of the interaction between the electron and the nuclei and their magnetic moment determines the distance between the splittings of the lines. This distance between the 1st and the 2nd peaks, describing the hyperfine splitting constant, is similar to the coupling constant J in NMR. It is labelled by the symbol a followed by a subscript indicating the splitting nucleus. Other parameters that could be easily obtained from the EPR spectra are the signal amplitude of the peaks (I) and the peak-to-peak line width (ΔB_{pp}) (Fig. 2). By them, the rotational correlation time (τ_c) can be calculated from the EPR

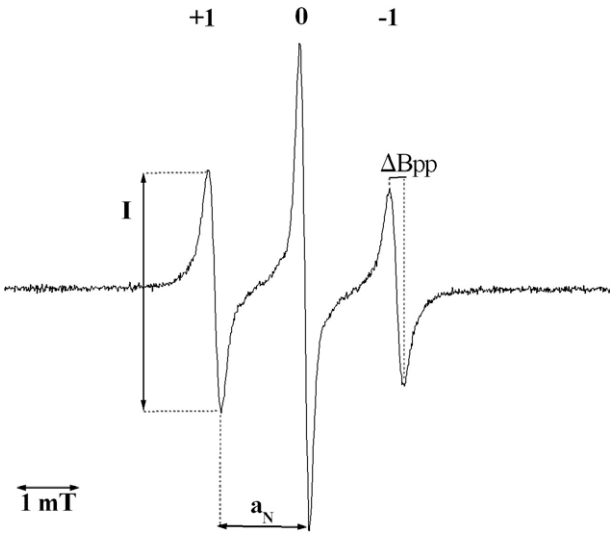

Fig. 2. EPR spectrum of AT (see structure 4 in Fig. 1) dissolved in PEG 400 illustrating typical EPR parameter: a_N – hyperfine splitting constant; I – signal amplitude; ΔB_{pp} – peak-to-peak line width.

spectrum [7]. EPR spectra are recorded usually in the form of the first derivative. Therefore, the signal intensity can be calculated by the double integration of the EPR spectra.

Molecular tumbling or molecular dynamics at a time scale between 10^{-10} s and 10^{-6} s induces relaxation processes, which influence the line width, the shape of the detected EPR lines and the spectral splitting at a time scale between 10^{-6} s and 10^{-3} s. So, the spectral splitting of the nitroxyl radicals is sensitive not only to the molecular motion and therefore the microviscosity of their surroundings, but also to the polarity of their direct environment. As mentioned earlier, the unpaired electron can be localized at the nitrogen atom, oxygen atom or ring structure of nitroxyl radicals. Only the nuclear spin of the nitroxyl nitrogen can contribute to the hyperfine splitting constant (a_N) of the EPR signal, when the radical is localized in the p_z-orbital of the nitrogen atom, because of the missing nuclear spin of the oxygen in the other mesomeric

form. Polar liquids (e.g. water) favour the existence of the mesomeric form at the nitrogen atom generating higher hyperfine splitting constants compared to apolar regions (e.g. oil) [5]. So, in the EPR spectra of the nitroxyl radical AT in water the distance between the outer lines is increased, compared to the oil MCT (middle chain triglycerides) (Fig. 3). The microviscosity, another parameter of the microenvironment strongly influences the tumbling behaviour of the nitroxyl radicals. In low viscous media they tumble freely, resulting in highly symmetric spectra with three narrow lines and rotational correlation times τ_c in the order of 0.01–0.1 ns (see EPR spectrum of the nitroxyl radical AT in water in Fig. 3). Increasing the viscosity decreases the molecular tumbling rate of the nitroxyl radical. Due to their restricted motion the anisotropy of the hyperfine interaction is only partially or not averaged, which results in a line broadening, a decrease in the signal amplitude and an increase in τ_c [8,9]. Like the chemical shift in NMR, the hyperfine interaction is anisotropic. In solution, anisotropic interactions are averaged out, and only the isotropic parts remain resulting in a higher spectral resolution and sensitivity. In solid material, the anisotropy is no longer averaged and typical "powder spectra" can be recorded (see EPR spectrum of AT in potato starch in Fig. 3). In the fast motional region, τ_c can be calculated from the ratio of amplitudes [10]. However, this method is limited to rotational correlation times shorter than 3 ns, and the calculation of τ_c from slow motion EPR spectra requires more specific mathematical operations [11].

Normally, the EPR spectrum is detected as a function of the magnetic field strength at a constant microwave frequency. Based on technical implementations, the EPR spectrum is plotted as a first derivative of the absorption spectrum. This first derivative is more sensitive to fast motional ("mobile") spin probes with their narrow isotropic line spectra. Superimposed spectra are a combination of the "mobile" with the "immobile" anisotropic spectrum; they are detectable at a rate below 1% [12].

Additionally, special nitroxide radicals permit the measurement of microacidity [13]. These nitroxyl radicals consist of additional functional groups (mostly amino-groups) in their molecule (see structures 4–6 in Fig. 1). Protonation of the amino-groups results in a decrease in the spin density at the nitroxyl nitrogen p-orbital resulting in a decrease in the hyperfine splitting (Fig. 4). The calibration curve of the pH dependency gives the expected sigmoid shape (Fig. 5), and as expected, the highest dependency occurs around the pK_a. Increasing differences between pH and pK_a decrease the response sensitivity. Moreover, the curve shows that the pH range that can be assessed ranges approximately from 2 to 3 units above and under the pK_a. There exist a wide range of stable nitroxide radicals with different pK_a values to cover the full pH range; and therefore, the measurement of more acidic and alkaline environments is possible. Recently developed nitroxides contain two protonable groups (structure 6 in Fig. 1), presenting two different pK_a values, so that a wider pH range can be covered by a single spin probe [14,15].

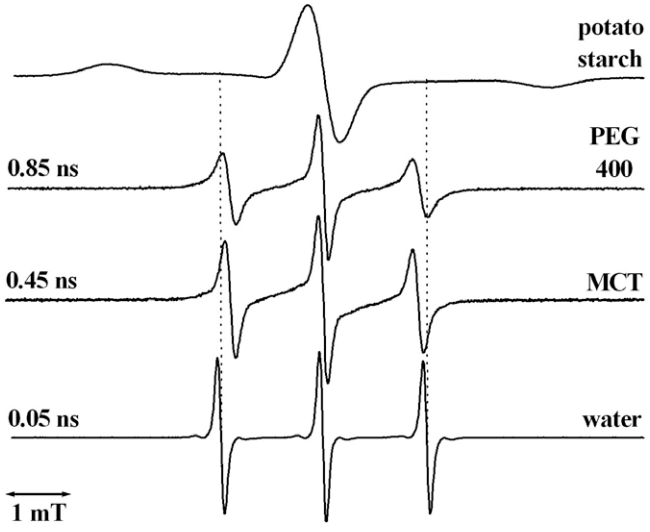

Fig. 3. EPR spectra of AT (see structure 4 in Fig. 1) in environments with different polarities and viscosities: potato starch, middle chain triglycerides (MCT), PEG 400 and water. The microviscosity of the spin probe environment is reflected by the corresponding rotational correlation times (τ_c): higher correlation times indicate lower tumbling rates and therefore higher microviscosities.

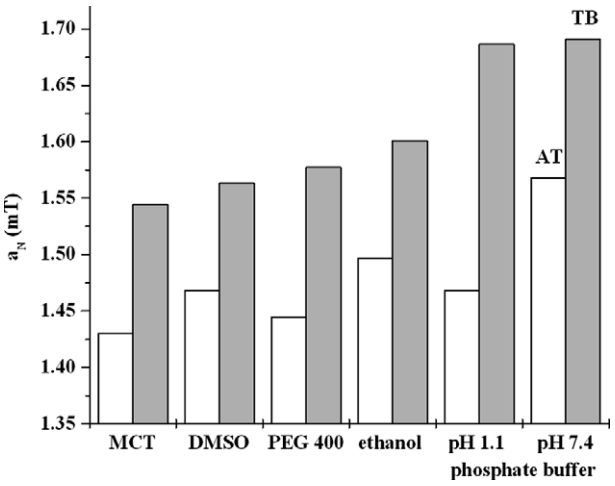

Fig. 4. Influence of environments with different polarities on the hyperfine splitting constant a_N of the pH-insensitive nitroxide Tempolbenzoate (TB-grey bars) and the pH-sensitive nitroxide AT (white bars). In regions with high polarity (e.g. water), the hyperfine splitting is increased compared to regions with low polarity, as in oil (MCT). Further, the pH-sensitive AT reflects acidic environments by a smaller hyperfine splitting.

Furthermore, there exists spin probes that are sensitive to the oxygen concentration. Oxygen itself is paramagnetic; however, it possesses a very broad EPR line due to the fast relaxation and is, therefore, not directly measurable at room temperature. Yet it interacts with other paramagnetic species causing additional oxygen concentration-dependent line broadenings. Recently, the group of Swartz provided a detailed overview about the oxygen measurements in tissues and *in vivo* including clinical applications of EPR oximetry [16].

2. Examples of pharmaceutical applications of EPR spectroscopy

EPR measurements can be divided into the direct measurement of radicals, as well as EPR spin trapping and EPR spin labelling techniques. We will mainly focus on drug delivery approaches and not discuss other applications such as the direct detection or trapping of radical metabolites, reactive oxygen species, nitric oxide or the determination of pO_2 by EPR oximetry [16–21].

EPR spectroscopy can be used to detect paramagnetic transition metals, such as Mn^{2+} and Fe^{3+}, down to the level of parts per million. The trace metals can be found in minerals (e.g. manganese(II) in talcum and bentonite), colour pigments or as impurities in excipients and active pharmaceutical ingredient (API) (Fig. 6). This species has the potential to catalyse the degradation of either excipients or API, so EPR can be used for the non-destructive identification and quantification of paramagnetic impurities [22].

Also, gamma irradiation during sterilisation processes may lead to the formation of stable or short living radicals which are detectable

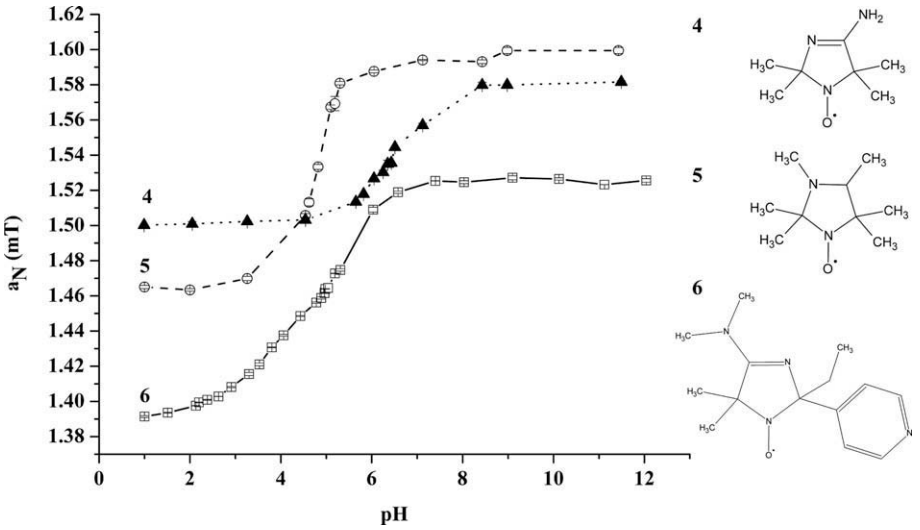

Fig. 5. pH sensitivity of the hyperfine splitting constant a_N of the nitroxides 4–6.

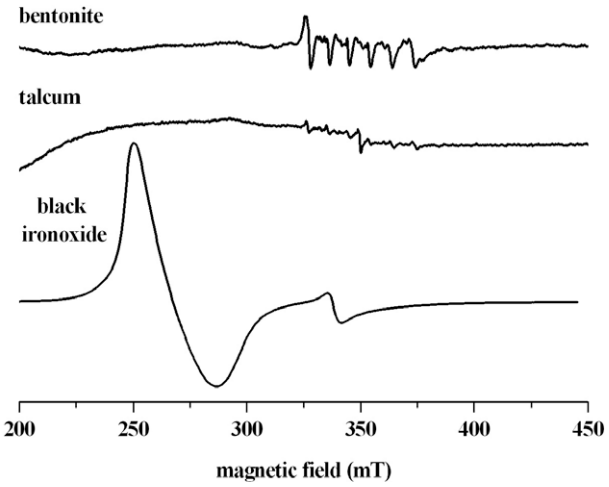

Fig. 6. EPR spectra of pharmaceutical excipients having intrinsic EPR active centres. Bentonite and talcum show manganese and iron signals. Whereas the EPR spectrum of black iron oxide (magnetite) is dominated by iron signal.

by EPR [23]. It is a widely used method of sterilisation for parenteral, polymer-based, controlled release formulations, such as poly(lactide-co-glycolide) (PLG) or poly(orthoester) [24,25]. The formed radicals may interact with incorporated drug molecules and therefore result in the degradation of the API. In addition, polymer degradation can occur, which may change the release and degradation kinetics or cause increased toxic by-products. Irradiation induced radicals might persist for very long times in dry solids (e.g. crystalline drugs or polymers). Therefore, they can be used as endogenous EPR signals to follow water penetration inside the polymers, because in the wet state the radicals disappear [26]. Otherwise, the detection of radiation induced radicals by EPR can be used to determine whether ingredients have explored irradiation treatment. Furthermore, the dose from radiation sterilised preparations can be estimated by re-irradiating the substances with defined doses and afterwards measuring the signal intensity [27].

However, the majority of drug delivery systems (DDS) are not detectable by EPR because they are diamagnetic and contain no paramagnetic molecules. They need the addition of exogenous stable free radicals as reporter molecules, so called spin probes. For example, there exist a large variety of commercially available stable nitroxyl radicals with different physicochemical properties, such as different hydrodynamic radius and HLB values. These spin probes can simulate a wide range of possible low molecular weight drugs (Fig. 1). Among them are spin probes with reactive functional groups, which can also be covalently linked to larger molecules such as proteins and polymers, by spin labelling. EPR allows the non-destructive measurement of non-transparent samples and can be applied to a wide range of dosage forms such as solids, solutions, suspensions, whole tablets and so on. From the EPR spectrum, we can get information about the radical concentration, the polarity of their direct environment, microviscosity and microacidity. Moreover, the spatial distribution of these parameters can be determined using spectral–spatial EPR imaging.

By the selection of appropriate spin probes (e.g. Tempolbenzoate "TB" see (2) in Fig. 1), it is possible to follow model drug distribution in multiphase systems at the molecular level. EPR can monitor directly and continuously the distribution of spin probes between hydrophilic and lipophilic environments in emulsions, nanodispersions, microemulsions, liposomes or self-assembling polymers [28–31]. Furthermore, one can the estimate drug loading capacities as it has been done for vesicular lipid dispersions or solid lipid nanoparticles (SLN). In SLN composed of 10% colloidal dispersion of glycerol behenate, the concentration of the lipophilic marker molecule TB inside the lipid matrix is low, as approximately 2/3 was pushed out onto the particle surface or into the aqueous phase due to the low incorporation of the spin probe into the lipid crystals. Whereas in colloidal dispersion of low concentrate amphiphilic sucrose ester (2%), about 94% of TB was entrapped in a lipophilic environment [28,29]. Other key parameters in the performance of colloidal drug carriers are the dynamics of distribution processes and their capacity to protect its contents against environmental changes. This protection capacity of drug delivery systems may be studied by ascorbic acid reduction assay, as ascorbic acid is localized in the aqueous phase and rapidly reduces e.g. accessible nitroxyl radicals to the EPR silent hydroxylamine. For nanocapsules, it was found that the spin probe reduction depends on the charge of the shell material and was faster for nanocapsules consisting of poly(D,L-lactide) PLA compared to pegylated PLA [32]. Colloidal systems undergo dilution both *in vitro* and *in vivo* after administration. This dilution process changes distribution equilibria which might cause a relocation of drugs. The determination of drug release in nanoscaled dispersions is not an easy

task, but the kinetics of such processes can be followed with spin probes as model drugs, rapidly and continuously measured without the need of sample separation. The relocation of the spin probe in the additional outer phase causes changes in the spectral shape. This dynamical process has been monitored for PLA nanocapsules by the distribution kinetics of the spin probe TB between the inner oily core of the nanocapsules and the outer water phase. Within one minute, 10% of the incorporate molecule diffused into the outer aqueous environment [32]. The fast distribution can be easily understood by the small shell thickness of about 10 nm, which provides nearly no diffusion barrier. *In vivo*, after oral administration, the drug distribution during fat digestion affects directly the absorption rate. EPR can follow the distribution of spin probes between water, oil and mixed micelles during *in vitro* lipolysis of olive oil and self-emulsifying drug delivery systems [33,34]. Moll et al. investigated the integrity of multilamellar liposomes after subcutaneous injection in mice [31]. For this purpose, they incorporated the nitroxide spin probe 2,2,6,6-tetramethyl-4-trimethylammoniumpiperidine-1-oxyl-iodide (CAT-1) inside the liposomes and detected its liberation by EPR spectroscopy. They could differentiate between encapsulated and released CAT-1 and show that the multilamellar liposomes forced a local depot after injection. The spin probe was released in a sustained manner from this depot. After 96 h, still 60% of CAT-1 remained in intact liposomes under the skin. No depot formation was observed for the pure CAT-1 solutions as the local signal intensity at the site of injection rapidly decreased due to systemic distribution and bioreduction of the nitroxide spin probe.

The detection of water penetration into solids as coated tablets, pellets or implants is another application to detect changes in micropolarity [35–37]. On Kollicoat SR/IR-coated tablets, it has been found that water was able to penetrate the coat rapidly and to dissolve the majority of an incorporated hydrophilic spin probe in the core within few minutes, despite the fact that the release process showed a lag time of several hours.

EPR permits also a deeper insight in the release mechanisms, because different release mechanisms cause different changes in the spectral shape. In diffusion-controlled release processes water penetration and solubilization lead to dramatic changes in the spectral shape. As mentioned earlier, the shape of an EPR spectrum might reflect the fast movements of spin probes in a system. In contrast, the spectral shape remains unchanged in pure erosion-controlled systems, and only the signal intensity will decrease, as shown for polyanhydrides [38]. In the majority of the drug delivery systems, diffusion plays a crucial role in the release process, and the spectral contributions from dissolved, rapidly tumbling radicals emerge and increase during the release process, for example, in proteineous matrices [39] or PLGA implants [37,38].

By using nitroxyl radicals of the both ^{14}N and ^{15}N isotopes, the simultaneous investigation of the release pattern of molecules with different lipophilicity or location is possible. The EPR spectra differ from each other due to the different nuclear spins. By means of this approach, it was possible to differentiate between inner and outer layers of PLGA as well as polyanhydride implants *in vitro* and *in vivo* [38]. Another example is the simultaneous monitoring of different probes in o/w-gelling systems: A hydrophilic spin probe (^{15}N-PCM) and a lipophilic spin probe (^{14}N-HD-PMI) were incorporated into in situ gelling chitosan-based emulsions as models for low molecular weight drugs (Fig. 7a). ^{15}N-PCM gives a typical 2-line spectrum. From the spectral shape and the hyperfine splitting, we can conclude that it is located in the aqueous environment of the gel (Fig. 7b). ^{14}N-HD-PMI shows a 3-line spectrum. Its spectral parameters indicate that ^{14}N-HD-PMI is dissolved in small oil droplets distributed within the chitosan backbone of the gel (Fig. 7b). Both spin labels had highly symmetric spectra with narrow lines indicating a high mobility inside the gels during the whole time of release (Fig. 8). Despite the formation of high viscous gels, the spin probes were located in a low viscous microenvironment. The release of the water soluble ^{15}N-PCM was completed after 6 h *in vitro* and after 3 h *in vivo*. As we can see the amplitudes decreased rapidly due to fast diffusion of ^{15}N-PCM out of the gels. In contrast, the spectra of ^{14}N-HD-PMI remained almost unchanged and were still detectable after 2 months *in vitro* and *in vivo*. The differences can be attributed to incomplete or slower gelation time *in vivo*. Other major differences to *in vitro* studies are decreased water availability and different pH values, buffer capacities or the involvement of enzymes. For the development of DDS, the correlation of *in vitro* and *in vivo* data is very important. EPR allows the non-invasive verification, if the drug release mechanisms and kinetics observed *in vitro* correspond to the *in vivo* situation in small animals, such as mice. A good *in vitro–in vivo* correlation was fund for the kinetic of N-methyl-pyrrolidine (NMP) water exchange and the velocity of polymer precipitation of in situ forming PLG/NMP implants [40]. On the other hand, for

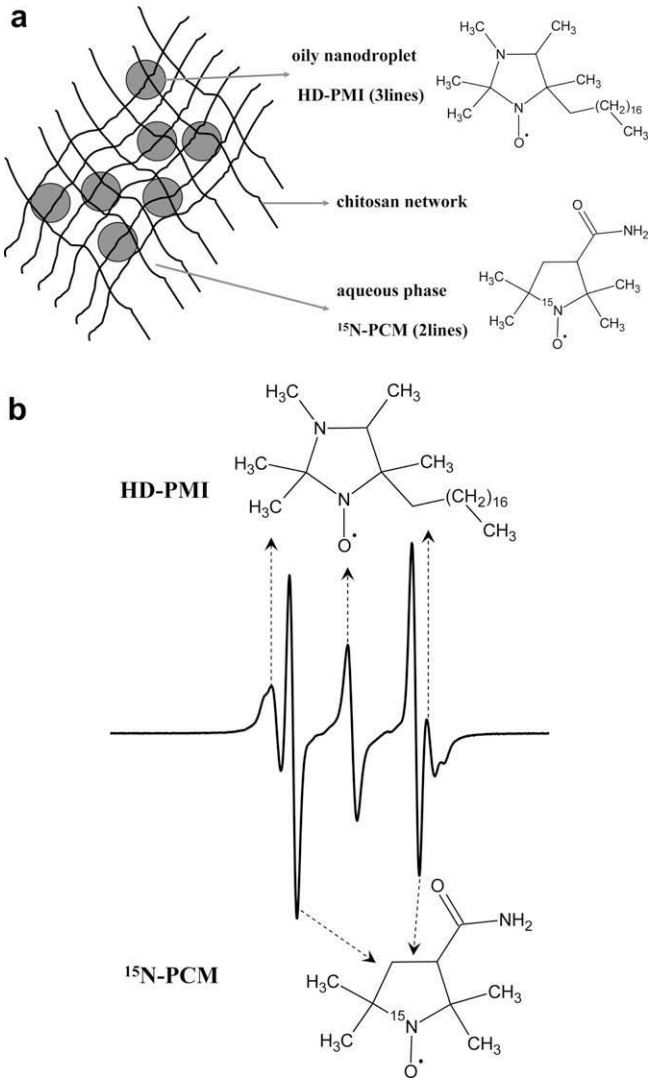

Fig. 7. (a) The principle of the simultaneous assessment of multiple sites of an oil/water chitosan-based in situ gelling emulsions by EPR. The lipophilic ^{14}N-nitroxide (HD-PMI) is localized in the oily nanodroplets, the ^{15}N-nitroxide (PCM) in the outer aqueous phase. (b) EPR spectrum of the ^{14}N-nitroxide (HD-PMI) and ^{15}N-nitroxide (PCM)-doped chitosan-based emulsion. The ^{14}N-nitrogen has a nuclear spin of 1, resulting in a three-line spectrum and the nuclear spin of ½ of the ^{15}N-nitrogen results in a hyperfine splitting of two lines. The outer line of the ^{14}N-hyperfine splitting is superimposed by the two lines of the ^{15}N-nitrogen.

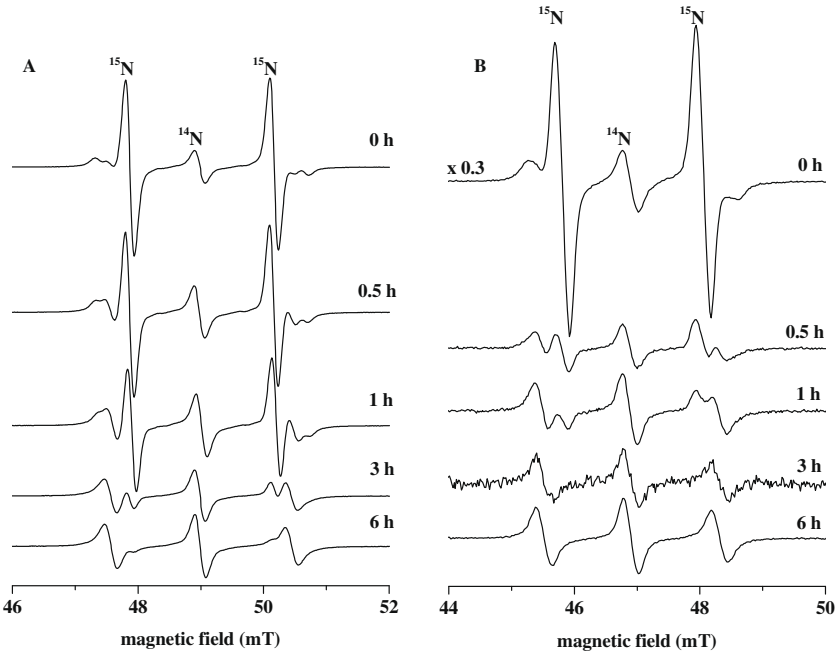

Fig. 8. *In vitro* (A) and *in vivo* (B) EPR spectra of ^{14}N-nitroxide (HD-PMI) and ^{15}N-nitroxide (PCM) in chitosan-based in situ gelling emulsions.

polyanhydrides, the *in vivo* release was 1.5 times slower compared to *in vitro* experiments [38]. EPR has also shown that spin probe release may be retarded *in vivo* due to encapsulation of implants [41], which might explain the observed incomplete drug release from these implants.

Not only nitroxyl radicals can be investigated as models for small molecule drugs but it is also possible to label drugs [8,42] or other components of drug delivery systems directly [43]. However, it has to be checked if the spin labelled product has similar or different physicochemical and pharmacological properties than the parent molecule. The differences can be considerable for small molecular weight drugs, but decrease with increasing molecular weight of the drug. Spin labelled drug molecules can give important information about their localization in the DDS and if they undergo changes during their release. It was shown that spin labelled insulin incorporated in thermosensitive chitosan gels was located in the aqueous environment of the gel and its rotational correlation time was comparable to a 2% solution in buffer. Quantitative analysis of the EPR spectra yielded that the gelation had no impact on the molecular mobility, despite the formation of high viscous gels. Within 2 weeks, the spin labelled insulin was released. The EPR spectra of the released insulin corresponded to EPR spectra of spin labelled insulin in the buffer system, suggesting that insulin is released without denaturation.

In drug delivery research, it is essential to determine the microenvironmental pH inside drug delivery systems during release periods. The pH value controls directly the stability of incorporated drugs, their solubility, release pattern and the degradation rate of polymers. Most commonly used biodegradable polymers such as polyhydroxyesters or polyorthoesters possess acidic monomers in their backbones. Upon incubation under physiological conditions, they hydrolyse into acidic oligomer and monomers. It has been shown that pH inside degrading PLGA implants might drop *in vivo* to acidic values as low as pH 2 [37]. Changes in the microacidity may also occur from the decomposition of hydrolysable drugs [44]. In addition to the incorporated drug, further ingredients like buffer substances or poorly soluble bases can influence microacidity. The pH inside degrading PLA microparticles was increased by adding sodium acetate [45]. Other examples for the EPR measurement of microacidity include the *in vitro* detection of pH gradients in tablets [46] and degrading polymers [47]. The depth specific tissue pH variation in human skin has been examined e*x vivo* after drug treatment [48]. The pH in the stomach and the gut was determined i*n vivo* after oral administration of nitroxide spin probes as well as the influence of co-administered antacid drugs [14,49,50].

3. Examples of pharmaceutical applications of EPR imaging

EPR imaging permits to monitor the spatial localization of paramagnetic molecules. By means of spectral–spatial EPR imaging, it is possible to record locally encoded EPR spectra. This technique is very helpful to monitor mobility, polarity or pH gradients that are important parameters for drug release processes. It is possible to perform EPR imaging at X-band (standard EPR, 9–10 GHz) or at L-band (1 GHz). X-band provides a better sensitivity and spatial resolution (about ten times), but it is difficult or impossible to perform with larger water-containing samples (e.g. hydrated tablets). The amount and the status of water determine whether or not X-band can be applied. It is possible to image isolated human or animal skin [51,52] or to characterize biodegradable polymers [53,54] by X-band EPR imaging.

In general, for EPR imaging, two main techniques exist: a rotating constant gradient (*cg*) and a variable gradient with a fixed orientation (*vg*). The latter is used in the case of 1D-spatial–spectral imaging, whereas the rotating gradients give 2D- or 3D-spatial images. The principles of both techniques can be illustrated with the following suggested experiment: You are taking photographs of a building from different positions. The first time (*cg*) you are going around the house with a constant distance and take photographs from different positions. The second time (*vg*) you are heading on a straight line for the building and are taking photographs from different distances. For both methods, different image reconstruction methods are necessary (back projection and FFT reconstruction or the Radon transformation). Using the constant gradient technique, the distribution and location of paramagnetic centres in a sample is obtained. A big disadvantage of the constant rotating gradient technique is the loss of the spectral information,

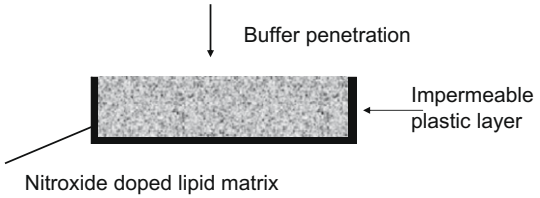

Fig. 9. Principle setup for 1D-spectral–spatial EPR imaging of lipid-based controlled release matrices.

which is necessary for the spatially resolved information of mobility, pH and polarity.

The spatial resolution depends on the ratio of the gradients to the line width of the ESR signal, which is typically lower in the L-band (100 μm to mm) and higher in the X-band (10 μm). The reason for the higher gradients in the X-band is the smaller distance between the gradient coils at constant current, because of the smaller dimension of the microwave resonator. Recently, advanced techniques have been introduced, which permit even higher resolutions, and EPR microscopy is now possible, but far from being a standard procedure [55].

1D-spectral–spatial EPR imaging gives 1D spatially resolved information about the spectral EPR features. Either the transformed backward fast Fourier transformation (FFT) or the filtered backward FFT are commonly used as reconstruction methods [56–59].

An example for the application of 1D-spectral–spatial L-band imaging is an EPR imaging study on lipid matrices for controlled release. Nitroxide spin probe-doped lipid matrices were molten into one side open flat cylinders (2 mm thickness, 8 mm diameter) and exposed to buffer solutions (Fig. 9). As illustrated, the buffer was only able to penetrate from the top. The samples were taken out of the buffer solution at dedicated time points and assessed by EPR imaging.

A typical spectral–spatial EPR contour plot is shown in Fig. 10. The axes have one spatial and one spectral component, the EPR signal intensity is colour coded. In contrast to EPR spectroscopy, the EPR contour plots are commonly displayed in the form of the absorption and not in the first derivative format.

It is now possible to take spectral or spatial cuts at different positions of these contour plots. The spatial cut represents intensity distributions of a certain spectral component at a definite position and from the spectral cut, information on mobility, polarity and (using special nitroxides) pH or oxygen can be obtained. Spectral–spatial EPR imaging, therefore, permits the detection of concentration, mobility, polarity and pH gradients within monolithic drug delivery systems.

It is well known that glycerol monooleate (GMO) forms in contact with water highly viscous cubic phases, which can be used for the controlled drug delivery. However, the knowledge is still limited concerning the kinetics of the hydration induced formation of the viscous cubic phase and the internal physicochemical properties (molecular viscosity and polarity). To shed more light on this topic, we incorporated 1 mmol Tempolbenzoate (TB) (^{14}N spin) and ^{15}N-nitroxide 3-carbamoyl-2,2,5 or 5-tetramethylpyrrolidine-1-oxyl (^{15}N-PCM) in the molten GMO as lipophilic (TB) and hydrophilic (PCM) model drugs (Fig. 11). The EPR Images display the spatial distribution of five lines. Three lines arise from the lipophilic nitroxide TB and two lines come from the hydrophilic spin probe ^{15}N-PCM. The central spatial cut is displayed on the right side, whilst exposure to the buffer leads to spectral and spatial changes. The spatial dimension is slightly increasing due to the swelling of the lipid; the EPR lines get narrower indicating more

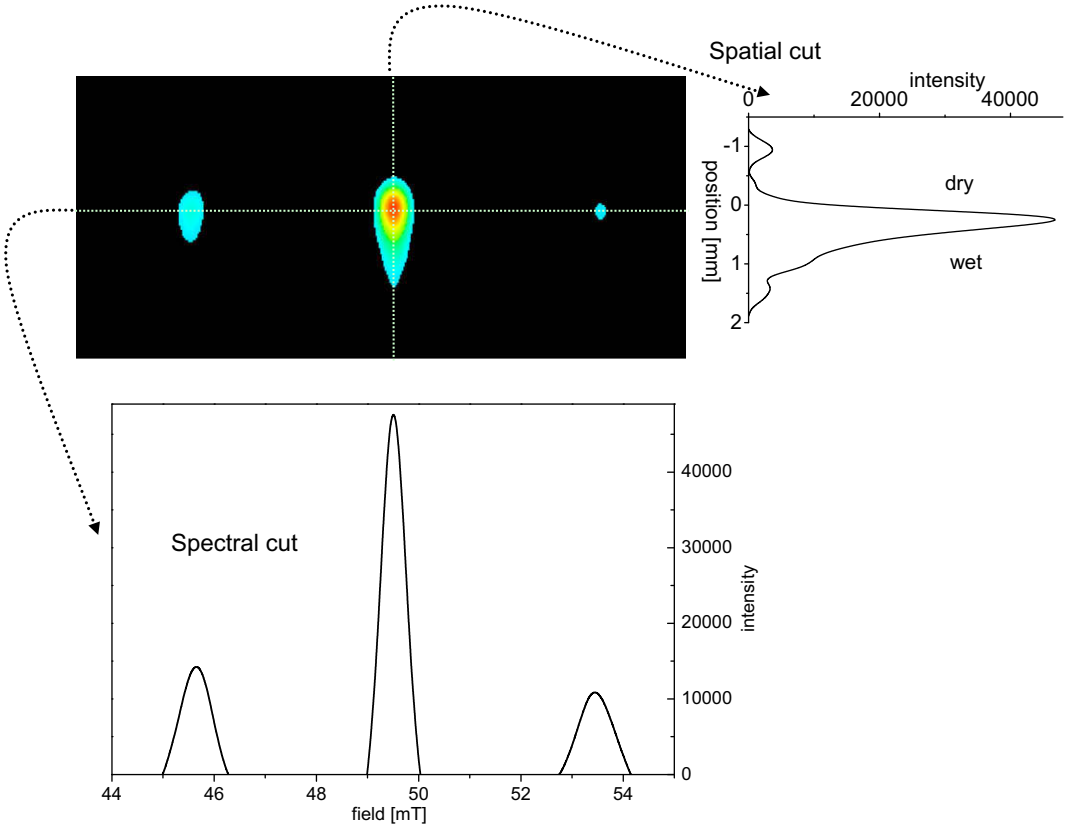

Fig. 10. Contour plot and spectral and spatial cuts of a nitroxide-loaded lipid matrix.

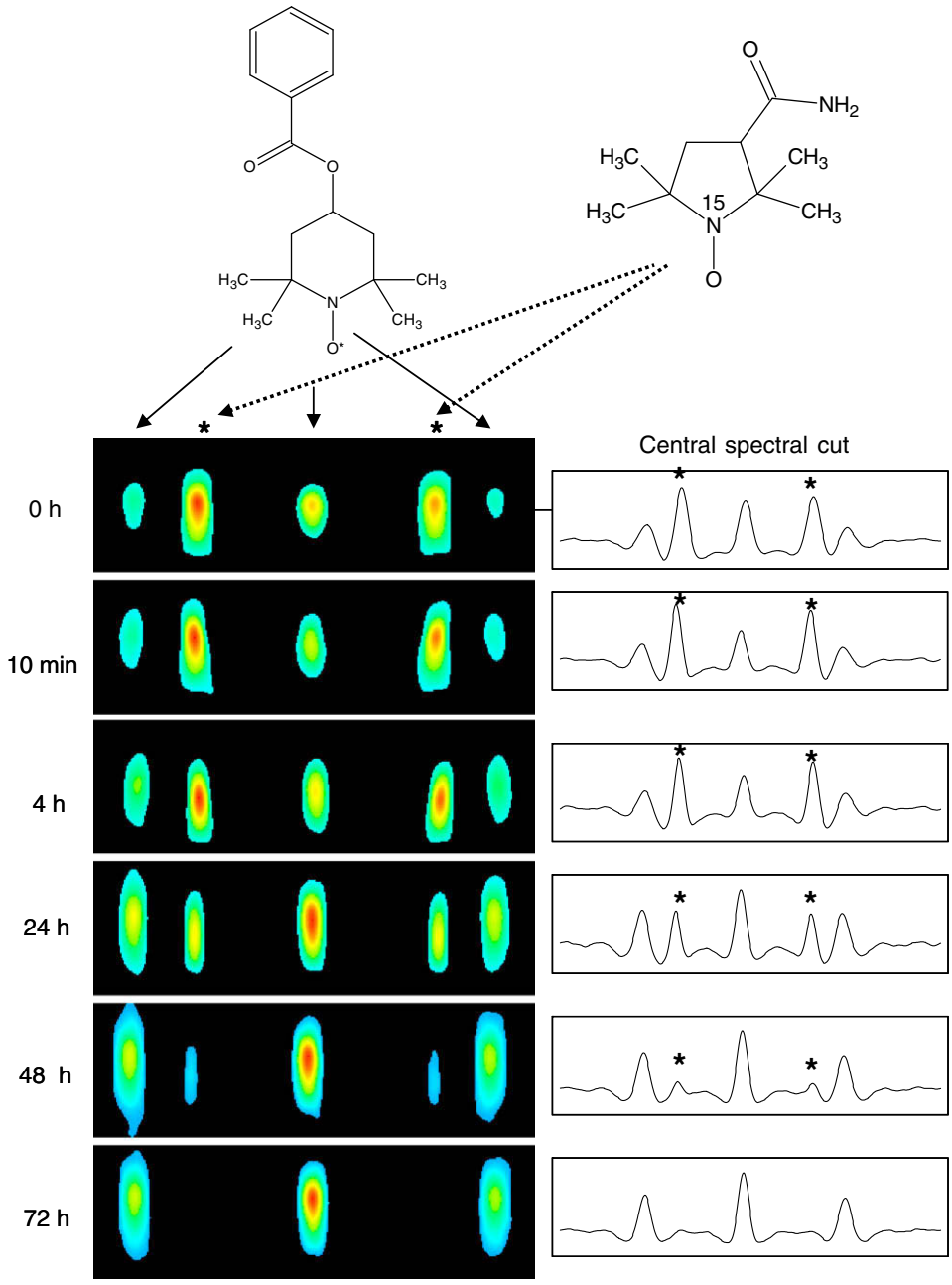

Fig. 11. Contour plot and central spectral cuts of Tempolbenzoate (TB) (^{14}N spin) and ^{15}N-nitroxide 3-carbamoyl-2,2,5 or 5-tetramethylpyrrolidine-1-oxyl (^{15}N-PCM)-loaded glycerol monooleate matrices before and after exposure to buffer.

mobility of the nitroxide due to a decreased viscosity. At the beginning, the signal amplitude of ^{15}N-PCM (marked by $*$) is higher compared to the three lines of TB. However, the amplitude ratio between the EPR signals changes with time and almost equal signal amplitudes are observed after 24 h. Only traces of ^{15}N-PCM are detected after 48 h. After 72 h, the release of the hydrophilic ^{15}N-PCM was complete and only the more hydrophobic TB remained in the swollen GMO lipid matrix.

In addition, we performed similar experiments with amphiphilic sucrose esters of fatty acids (SE). SE are very versatile excipients, which have a long history in the food and cosmetic industry, but recently they have became more important in the pharmaceutical market. They cover a broad range of different HLB values and are alternative matrices for peroral-controlled drug delivery products. Although SE-based Ibuprofen-controlled release tablets are on the market, little is known about the detailed mechanism of drug release. The amphiphilic sucrose ester S1170 (HLB value 11, fatty acids consist of 70% stearate and the residue is mainly palmitate) was doped with the hydrophilic nitroxide Tempol and exposed to buffer as indicated in Fig. 9. The EPR images are displayed in Fig. 12.

Three spectral cuts (A–C) are displayed for each time point. B represents the central layer. A is 0.5 mm more closely localized to the surface and C represents a layer which is 0.5 mm below the central layer. Because the buffer penetrates only from the top, it will reach first layer A, followed by B and C. Compared to GMO, the nitroxides are more immobilised in the dry lipid matrix, which results in anisotropic EPR spectra. Therefore, only the central EPR line is visible in the dry lipid matrix. Even after 5 days, the hydrophilic molecule Tempol can be detected in the SE matrix, whereas it was released from GMO within 3 days. Therefore, the

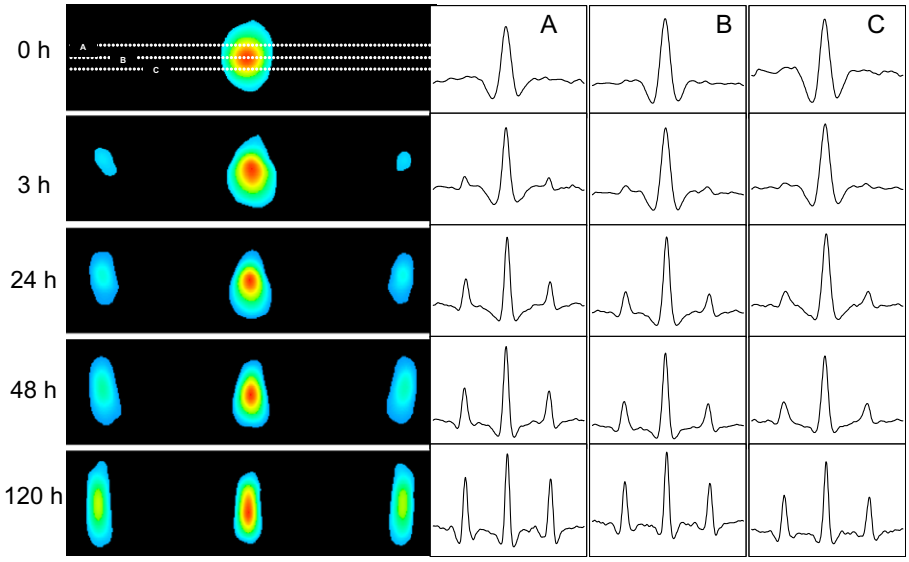

Fig. 12. Contour plot and spectral cuts from different layers of a Tempol (4-hydroxy-2,2,6,6-tetramethyl-piperidin-1-oxyl)-loaded sucrose ester matrix.

drug release rate for hydrophilic compounds is slower for the investigated SE ester-based matrix.

As expected, no spectral differences are observed between A, B, C at the start of the experiment. However, after 3 h, the contour plot and the spectral cuts have changed in the upper, but not in the deeper layers (Fig. 12; 3 h). Two other signal intensities emerge in addition to the central line. This change indicates that a small percentage of the Tempol molecules in the upper layer are in the mobile state due to solubilization by water.

In time, more and more Tempol molecules were solubilized, so the amplitude of the outer peaks increased. The amplitude ratio of central line/third line is decreasing with increasing time, and for a fully solubilized nitroxide in a low viscous environment, it would be close to one. The solubilization front advances from the top and reaches the bottom after 2 days. On the top side, which was exposed to the buffer, the spectral line is noticeably smaller because of the higher mobility of the molecules in the moisture expansion of the sucrose ester [60]. However, the degree of solubilization is still increasing, and the outer lines increase in their amplitude. The spectral cuts indicate also that for all time points after buffer exposure (including 120 h), the percentage of solubilized molecules is higher in the top layers compared to the bottom layers. As already discussed, the hyperfine splitting a_N depends on the polarity of the environment [5,61]. From the hyperfine splitting of the spectral cuts, hyperfine profiles can be calculated for each time point as illustrated in Fig. 13. The results indicate that (i) the polarity gradients exist within the SE matrix, (ii) the polarity is increasing with time, (iii) and after several days, Tempol molecules localized in the outer layers are dissolved in an environment with a polarity comparable to the surrounding buffer.

In a similar way to the GMO and SE-based lipid systems, EPR imaging was used to characterize release processed from high molecular weight PEG-based Egalet® tablets. The polarity gradient, the spatial intensity profiles and the release kinetics of the TEMPOL were analysed [62].

As an alternative option to drug-loaded delivery systems, a hydrophilic spin probe like TEMPOL or other nitroxides can be dissolved in the release medium. By EPR imaging, it is now possible to follow the diffusion of these molecules from the buffer into the tablet or implant. By variation of the molecular weight and the charge of the nitroxides, it is possible to detect which molecules are able to penetrate as well as discovering their penetration kinetics.

In addition to spectral–spatial EPR imaging, it is also possible to perform 2D- or 3D-spatial imaging. An example for a 3D Image of a DPPH-loaded, controlled release tablet before and after 24 h exposure to buffer is given in Fig. 14.

What are the current limitations and future perspectives of EPR imaging? Despite the progress that has been made, EPR imaging is still scarcely used to for the characterization of drug delivery processes. The main problems are:

(1) Long measurement times.
(2) Insufficient signal intensity.
(3) Possible artefacts.

The main reasons for these limitations are the limited sensitivity of low frequency EPR machines, the limitations of the EPR imaging hard and software as well as the undesirable properties of many spin probes.

The sensitivity of the spectrometer has been improved over the years. Low frequency EPR is intrinsically less sensitive to higher EPR frequency due to the laws of magnetic resonance, but hydrated tablets and small animals can only be measured at this frequency range. Progress has also been made with the hardware and software,

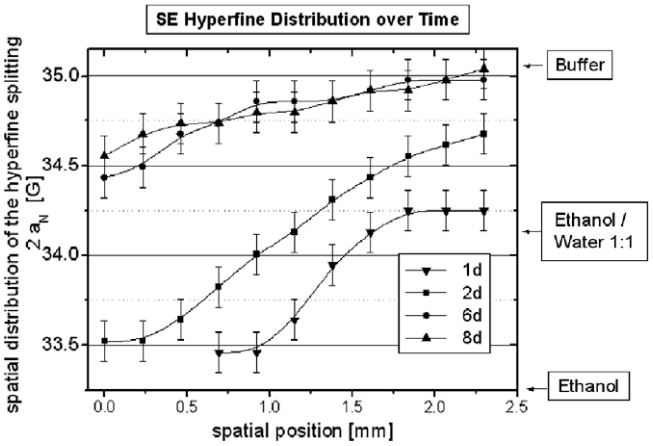

Fig. 13. Spatially resolved polarity profile of the Tempol-loaded sucrose ester matrices. Higher hyperfine splittings represent a higher polarity. With time, the overall polarity is increasing and the gradient decreasing.

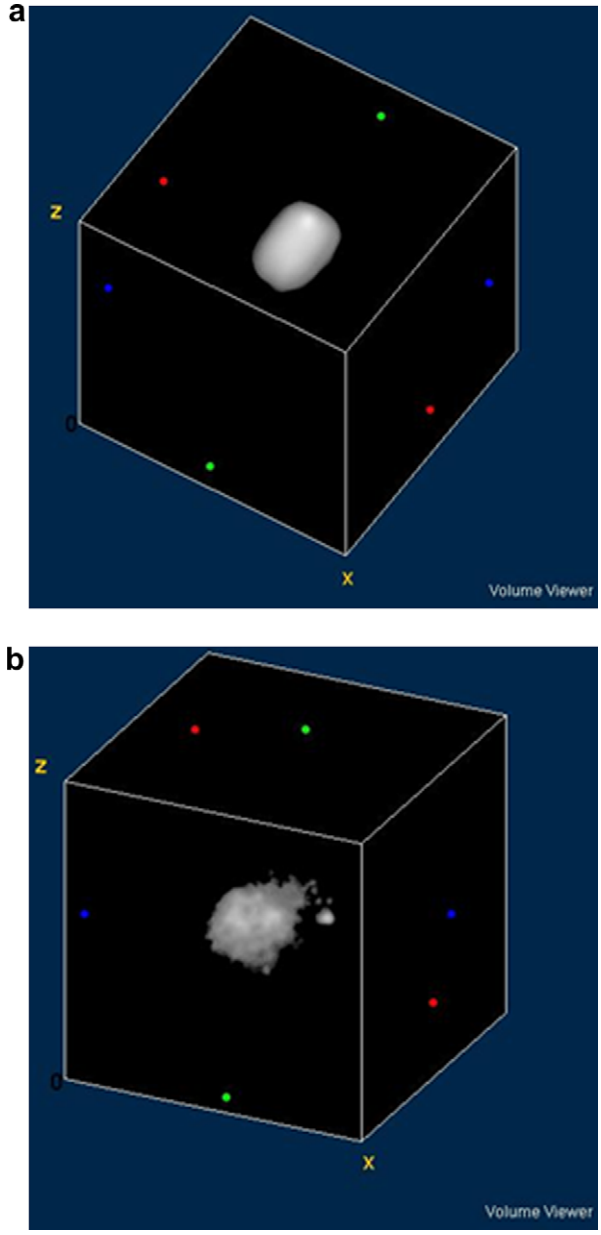

Fig. 14. 3D-spatial EPR Image of a DPPH-loaded tablet before (a) and after (b) 24-h exposure to buffer.

although worldwide only a small, but increasing number of scientists are working on this field. The largest potential for EPR imaging (and also *in vivo* spectroscopy) has the development of new spin probes. This statement is based on the following facts. The spatial resolution depends on the ratio between the maximal gradient strength and the width of the indispensable spectral field range named sweep. For a large sweep, the volume elements, which are in resonance, are smaller, the spatial resolution is higher but the number of unpaired electrons and the signal strength decrease. It is indispensable to find a compromise between both oppositional influences. For nitroxide spin probes, a sweep of 8 mT is a good choice and results in a gradient of 2.16 mT/cm. For a sweep of 4 mT, the signal intensity is more than three times higher, but the spatial resolution is not as good. Spin probes with narrow lines have more signal amplitude and permit higher resolution.

The EPR line width of nitroxyl radicals is also influenced by the interaction with the nuclear spins of distant atoms (called superhyperfine coupling). For nitroxide spin probes, deuteration of the methyl groups reduces this broadening effect by a factor of 6.5. Therefore, for deuterated spin probes, the EPR line widths are about six times smaller (this value also depends on the tumbling rate), and in the case of the same concentration, the signal amplitude is much higher. However, deuterated nitroxides are expensive. Signal amplitude can be further enhanced slightly by using ^{15}N- instead of ^{14}N-nitroxides but again, this makes EPR more expensive and only a few compounds are commercially available. In addition, the existence of several EPR lines might cause artefacts in some EPR imaging procedures. Moreover, there are some trails to overcome this problem with the help of mathematics. The splitting of the EPR lines can be theoretically explained as a convolution of a line shape function with one extremely sharp line. This line shape function can be measured as a conventional EPR spectrum. There were several attempts to develop a deconvolution algorithm [63,64], and this theoretical option was unfortunately successful only in a few cases in practice.

However, EPR spin probes with one extremely small line would be the best choice for 2D- and 3D-spatial imaging, because they permit a high resolution at decreased measurement times and avoid artefacts. Such stable radicals exist and have been recently developed. Hydrophilic and lipophilic derivatives of triarylmethyl radicals (TAM) have been synthesized and have shown superior properties for *in vivo* EPR oximetry, although (compared to nitroxides) they are commonly less useful to monitor polarity and pH [65–67]. Originally, TAM structures have been developed by Nycomed for dynamic nuclear polarization (DNP) in the NMR. They are now used *in vitro* and *in vivo* for DNP. Unfortunately, TAM structures are not commercially available, which limits the spread of these materials and the success of EPR imaging. The disadvantage of TAM-type radicals is the loss of spectral information (hyperfine splitting). Therefore, the influence of pH, polarity and microviscosity can only be analysed by investigating line width effects of the single EPR line. This method is not as sensitive as the analysis of the hyperfine splitting of the nitroxide radicals. Alternative materials are lithium-doped phthalocyanine and related structures [68–73], but unfortunately these are not available commercially. Furthermore, it is unfortunate that the current use of EPR imaging is not only limited by the small number of EPR imaging machines, which do exist, but also by the access to the superior EPR probes with a single narrow line.

4. Summary and outlook

EPR spectroscopy and imaging is an analytical method, which requires the presence of paramagnetic species which permits the touchless, non-invasive and continuous measurement of solid, liquid or gaseous samples. EPR can be applied to non-transparent samples, including small animals or skin-deep layers of humans. In most cases, paramagnetic markers have to be introduced into the samples, which serve as local reporters of the microviscosity, micropolarity and (using special probes) pH. This information yields new insights into drug delivery processes taking place *in vitro* and *in vivo*. Further exciting applications arise from the possibility of measuring oxygen concentrations.

The appropriate selection of the nitroxide or alternative paramagnetic probes, their concentration and the measurement parameters are a prerequisite for meaningful results. In the case of pH measurements, control experiments with pH-insensitive nitroxides should be carried out to exclude that polarity or ion effects cause the observed "pH" change, as they do also influence the hyperfine splitting. Further studies need to be done to explore the power of EPR for the determination of the "microacidity" on or in solids.

Multiple species (e.g. hydrophilic and hydrophobic model drugs, high and low molecular weight model drugs) can be observed simultaneously taking advantage of different nitrogen isotopes.

EPR imaging permits the spatially resolved measurement of polarity, viscosity and pH gradients. Using these approaches, EPR provides unique information on drug release mechanisms and kinetics.

Exciting possibilities have been shown in the field of *in vivo* EPR measurements on small mammals. *In vivo* applications are mainly limited by the problems of a decreased sensitivity. However, the current development of new probes (not nitroxide based) with a single line and a narrow line width opens the door to overcome this problem. It is, therefore, fair to predict that *in vivo* EPR imaging will become more and more important as an interesting technique to monitor the distribution and the physicochemical state of drug delivery systems *in vivo*, including nanoscaled drug delivery systems.

Acknowledgement

We gratefully thank Sarah Ruth Brownlee for their contribution to finalize the manuscript.

References

[1] E. Zavoiskii, Paramagnetic absorption of a solution in parallel fields, Journal of Physics 8 (1944) 377–380.
[2] J.A. Weil, J.R. Bolton, Electron Paramagnetic Resonance – Elementary Theory and Practical Applications, second ed., John Wiley & Sons, Hoboken, New Jersey, 2007.
[3] N.M. Atherton, Principles of Electron Spin Resonance, Ellis Horword PTR, Prentice Hall, New York, 1993.
[4] W. Gordy, Theory and Applications of Electron Spin Resonance, Wiley & Sons, New York, 1980.
[5] D.J. Lurie, K. Mäder, Monitoring drug delivery processes by EPR and related techniques – principles and applications, Advanced Drug Delivery Reviews 57 (2005) 1171–1190.
[6] M. Carini, G. Aldini, M. Orioli, R.M. Facino, Electron paramagnetic resonance (EPR) spectroscopy: a versatile and powerful tool in pharmaceutical and biomedical analysis, Current Pharmaceutical Analysis 2 (2006) 141–159.
[7] S. Lüsse, K. Arnold, Water binding of polysaccharides – NMR and ESR studies, Macromolecules 31 (1998) 6891–6897.
[8] A. Besheer, K.M. Wood, N.A. Peppas, K. Mäder, Loading and mobility of spin-labeled insulin in physiologically responsive complexation hydrogels intended for oral administration, Journal of Controlled Release 111 (2006) 73–80.
[9] K. Mäder, B. Bittner, Y.X. Li, W. Wohlauf, T. Kissel, Monitoring microviscosity and microacidity of the albumin microenvironment inside degrading microparticles from poly(lactide-co-glycolide) (PLG) or ABA-triblock polymers containing hydrophobic poly(lactide-co-glycolide) A blocks and hydrophilic poly(ethyleneoxide) B blocks, Pharmaceutical Research 15 (1998) 787–793.
[10] R.G. Evans, A.J. Wain, C. Hardcare, R.G. Compton, An electrochemical and ESR spectroscopic study on the molecular dynamics of TEMPO in room temperature ionic liquid solvents, ChemPhysChem 6 (2005) 1035–1039.
[11] D.E. Budil, S. Lee, S. Saxena, J.H. Freed, Nonlinear-least-squares analysis of slow-motion EPR spectra in one and two dimensions using a modified Levenberg–Marquardt algorithm, Journal of Magnetic Resonance, Series A 120 (1996) 155–189.
[12] K. Mäder, Characterization of Nanoscaled Drug Delivery Systems by Electron Spin Resonance (ESR), Nanosystem Characterization Tools in the Life Science, Wiley-VCH, Weinheim, 2006. pp. 241–258.
[13] V.V. Khramtsov, Biological imaging and spectroscopy of pH, Current Organic Chemistry 9 (2005) 909–923.
[14] D.I. Potapenko, M.A. Foster, D.J. Lurie, I.A. Kirilyuk, J.M.S. Hutchison, I.A. Grigor'ev, E.G. Bagryanskaya, V.V. Khramtsov, Real-time monitoring of drug-induced changes in the stomach acidity of living rats using improved pH-sensitive nitroxides and low-field EPR techniques, Journal of Magnetic Resonance 182 (2006) 1–11.
[15] I.A. Kirilyuk, A.A. Bobko, V.V. Khramtsov, I.A. Grigor'ev, Nitroxides with two p*K* values – useful spin probes for pH monitoring within a broad range, Organic & Biomolecular Chemistry 3 (2005) 1269–1274.
[16] N. Khan, B.B. William, H. Hou, H. Li, H.M. Swartz, Repetitive tissue pO_2 measurements by electron paramagnetic resonance oximetry: current status and future potential for experimental and clinical studies, Antioxidants & Redox Signaling 9 (2007) 1169–1182.
[17] A.A. Bobko, E.G. Bagryanskaya, V.A. Reznikov, N.G. Kolosova, T.L. Clanton, V.V. Khramtsov, Redox-sensitive mechanism of NO scavenging by nitronyl nitroxides, Free Radical Biology and Medicine 36 (2004) 248–258.
[18] B. Gallez, C. Baudelet, B.F. Jordan, Assessment of tumor oxygenation by electron paramagnetic resonance: principles and applications, NMR in Biomedicine 17 (2004) 240–262.
[19] B.F. Jordan, P. Sonveaux, O. Feron, V. Gregoire, N. Beghein, C. Dessy, B. Gallez, Nitric oxide as a radiosensitizer: evidence for an intrinsic role in addition to its effect on oxygen delivery and consumption, International Journal of Cancer 109 (2004) 768–773.
[20] K. Mäder, G. Bacic, H.M. Swartz, In vivo detection of anthralin-derived free-radicals in the skin of hairless mice by low-frequency electron-paramagnetic-resonance spectroscopy, Journal of Investigative Dermatology 104 (1995) 514–517.
[21] Y. Yoshimura, T. Inomata, H. Nakazawa, H. Kubo, F. Yamaguchi, T. Ariga, Evaluation of free radical scavenging activities of antioxidants with an H_2O_2/NaOH/DMSO system by electron spin resonance, Journal of Agriculture and Food Chemistry 47 (1999) 4653–4656.
[22] H.E. Williams, V.C. Loades, M. Claybourn, D.M. Murphy, Electron paramagnetic resonance spectroscopy studies of oxidative degradation of an active pharmaceutical ingredient and quantitative analysis of the organic radical intermediates using partial least-squares regression, Analytical Chemistry 78 (2006) 604–608.
[23] K.G. Desai, H.J. Park, Study of gamma-irradiation effects on chitosan microparticles, Drug Delivery 13 (2006) 39–50.
[24] M.B. Sintzel, K. Schwach-Abdellaoui, K. Mäder, R. Stosser, J. Heller, C. Tabatabay, R. Gurny, Influence of irradiation sterilization on a semi-solid poly(ortho ester), International Journal of Pharmaceutics 175 (1998) 165–176.
[25] J.A. Bushell, M. Claybourn, H.E. Williams, D.M. Murphy, An EPR and ENDOR study of γ- and β-radiation sterilization in poly(lactide-co-glycolide) polymers and microspheres, Journal of Controlled Release 110 (2005) 49–57.
[26] K. Mäder, A. Domb, H.M. Swartz, Gamma-sterilization-induced radicals in biodegradable drug delivery systems, Applied Radiation and Isotopes 47 (1996) 1669–1674.
[27] J.P. Basly, I. Basly, M. Bernard, ESR spectroscopy applied to study of pharmaceuticals radiosterilization: cefoperazone, Journal of Pharmaceutical Sciences 17 (1998) 871–875.
[28] K. Jores, W. Mehnert, K. Mäder, Physicochemical investigations on solid lipid nanoparticles and on oil-loaded solid lipid nanoparticles: a nuclear magnetic resonance and electron spin resonance study, Pharmaceutical Research 20 (2003) 1274–1283.
[29] S. Ullrich, H. Metz, K. Mäder, Sucrose ester nanodispersions: microviscosity and viscoelastic properties, European Journal of Pharmaceutics and Biopharmaceutics 70 (2008) 550–555.
[30] W. Herrmann, R. Stösser, H.H. Borchert, ESR imaging investigations of two-phase systems, Magnetic Resonance in Chemistry 45 (2007) 496–507.
[31] K.P. Moll, R. Stösser, W. Herrmann, H.H. Borchert, H. Utsumi, In vivo ESR studies on subcutaneously injected multilamellar liposomes in living mice, Pharmaceutical Research 21 (2004) 2017–2024.
[32] A. Rübe, K. Mäder, Electron spin resonance study on the dynamics of polymeric nanocapsules, Journal of Biomedical Nanotechnology 1 (2005) 208–213.
[33] A. Abdalla, K. Mäder, ESR studies on the influence of physiological dissolution and digestion media on the lipid phase characteristics of SEDDS and SEDDS pellets, International Journal of Pharmaceutics 367 (2009) 29–36.
[34] A. Rübe, S. Klein, K. Mäder, Monitoring of in vitro fat digestion by electron paramagnetic resonance spectroscopy, Pharmaceutical Research 23 (2006) 2024–2029.
[35] S. Strübing, H. Metz, K. Mäder, Mechanistic analysis of drug release from tablets with membrane controlled drug delivery, European Journal of Pharmaceutics and Biopharmaceutics 66 (2007) 113–119.
[36] A. Abdalla, K. Mäder, Preparation and characterization of a self-emulsifying pellet formulation, European Journal of Pharmaceutics and Biopharmaceutics 66 (2007) 220–226.
[37] K. Mäder, B. Gallez, K.J. Liu, H.M. Swartz, Non-invasive in vivo characterization of release processes in biodegradable polymers by low-frequency electron paramagnetic resonance spectroscopy, Biomaterials 17 (1996) 457–461.
[38] K. Mäder, G. Bacic, A. Domb, O. Elmalak, R. Langer, H.M. Swartz, Noninvasive in vivo monitoring of drug release and polymer erosion from biodegradable polymers by EPR spectroscopy and NMR imaging, Journal of Pharmaceutical Sciences 86 (1997) 126–134.
[39] I. Katzhendler, K. Mäder, M. Friedman, Correlation between drug release kinetics from proteineous matrix and matrix structure: EPR and NMR study, Journal of Pharmaceutical Sciences 89 (2000) 365–381.
[40] S. Kempe, H. Metz, K. Mäder, Do in situ forming PLG/NMP implants behave similar in vitro and in vivo? A non-invasive and quantitative EPR investigation on the mechanism of the implant formation process, Journal of Controlled Release 130 (2008) 220–225.
[41] K. Mäder, Y. Cremmilleux, A.J. Domb, J.F. Dunn, H.M. Swartz, In vitro in vivo comparison of drug release and polymer erosion from biodegradable P(FAD-SA) polyanhydrides – a noninvasive approach by the combined use of electron paramagnetic resonance spectroscopy and nuclear magnetic resonance imaging, Pharmaceutical Research 14 (1997) 820–826.
[42] J. Kristl, J. Smid-Korbar, E. Struc, M. Shara, H. Rupprecht, Hydrocolloids and gels of chitosan as drug carriers, International Journal of Pharmaceutics 99 (1993) 13–19.

[43] A. Besheer, K. Mäder, S. Kaiser, J. Kressler, C. Weiss, D. Oelkrug, Tracking of urinary excretion of high molar mass poly(vinyl alcohol), Journal of Biomedical Materials Research Part B – Applied Biomaterials 82B (2007) 383–389.
[44] C. Kroll, K. Mäder, R. Stosser, H.H. Borchert, Direct and continuous determination of pH values in nontransparent W/O systems by means of EPR spectroscopy, European Journal of Pharmaceutical Sciences 3 (1995) 21–26.
[45] A. Brunner, K. Mäder, A. Göpferich, pH and osmotic pressure inside biodegradable microspheres during erosion, Pharmaceutical Research 16 (1999) 847–853.
[46] S. Siepe, W. Herrmann, H.H. Borchert, B. Lueckel, A. Kramer, A. Ries, R. Gurny, Microenvironmental pH and microviscosity inside pH-controlled matrix tablets: an EPR imaging study, Journal of Controlled Release 112 (2006) 72–78.
[47] K. Mäder, S. Nitschke, R. Stosser, H.H. Borchert, A. Domb, Non-destructive and localized assessment of acidic microenvironments inside biodegradable polyanhydrides by spectral spatial electron paramagnetic resonance imaging, Polymer 38 (1997) 4785–4794.
[48] C. Kroll, W. Herrmann, R. Stösser, H.H. Borchert, K. Mäder, Influence of drug treatment on the microacidity in rat and human skin – an in vitro electron spin resonance imaging study, Pharmaceutical Research 18 (2001) 525–530.
[49] B. Gallez, K. Mäder, H.M. Swartz, Noninvasive measurement of the pH inside the gut by using pH-sensitive nitroxides. An in vivo EPR study, Magnetic Resonance in Medicine 36 (1996) 694–697.
[50] M.A. Foster, I.A. Grigor'ev, D.J. Lurie, V.V. Khramtsov, S. McCallum, I. Panagiotelis, J.M.S. Hutchison, A. Koptioug, I. Nicholson, In vivo detection of a pH-sensitive nitroxide in the rat stomach by low-field ESR-based techniques, Magnetic Resonance in Medicine 49 (2003) 558–567.
[51] K.P. Moll, W. Herrmann, R. Stosser, H.H. Borchert, Changes of the properties in the upper layers of human skin on treatment with models of different pharmaceutical formulations – an ex vivo ESR imaging study, ChemMedChem 3 (2008) 653–659.
[52] T. Herrling, J. Fuchs, N. Groth, Kinetic measurements using EPR imaging with a modulated field gradient, Journal of Magnetic Resonance 154 (2002) 6–14.
[53] K. Mäder, R. Stosser, H.H. Borchert, R. Mank, B. Nerlich, EPR-studies of the penetration of water into polymer foils and microparticles on the base of biodegradable polyesters, Pharmazie 46 (1991) 342–345.
[54] K. Mäder, S. Nitschke, R. Stösser, H.H. Borchert, A. Domb, Non-destructive and localized assessment of acidic microenvironments inside biodegradable polyanhydrides by spectral spatial electron paramagnetic resonance imaging, Polymer 38 (1997) 4785–4794.
[55] A. Blank, J.H. Freed, C.H. Wang, Electron spin resonance microscopy applied to the study of controlled drug release, Journal of Controlled Release 111 (2009) 174–184.
[56] M.J.R. Hoch, Electron spin resonance imaging of paramagnetic centres in solids, Journal of Physical Chemistry 14 (1981) 5659–5666.
[57] M. Sueki, G.R. Eaton, S.S. Eaton, Multidimensional EPR imaging of nitroxides, Pure Applied Chemistry 62 (1990) 229–234.
[58] M.M. Maltempo, S.S. Eaton, G.R. Eaton, Spectral–spatial imaging, in: G.R. Eaton, S.S. Eaton, K. Ohno (Eds.), EPR Imaging and In Vivo EPR, vol. 14, CRC Press Inc., Boston, 2008, pp. 135–143.
[59] S.S. Eaton, G.R. Eaton, EPR Imaging, Electron Paramagnetic Resonance, vol. 17, Thomas Graham House, Cambridge, UK, 2000, pp. 109–129.
[60] H. Metz and K. Mäder, Spectral–spatial EPR Imaging of drug delivery systems, in: EPR 2005, Columbus, Ohio, USA, 2005, p. 130.
[61] A. Sotgiu, K. Mäder, G. Placidi, S. Colacicchi, C.L. Ursini, M. Alecci, pH-sensitive imaging by low-frequency EPR: a model study for biological applications, Physics in Medicine and Biology 43 (1998) 1921–1930.
[62] H. Metz, D. Bar-Shalom, H. Hemmingsen, G. Fischer, K. Mäder, PR and NMR Imaging in monitoring the release mechanisms from EGALET dossage units, 33rd Annual Meeting and Exposition of the Controlled Release Society Vienna, Austria, 2006.
[63] A. Sotgiu, D. Gazzillo, F. Momo, ESR imaging: spatial deconvolution in the presence of an asymmetric hyperfine structure, Journal of Physics C: Solid State Physics 20 (1987) 6297–6340.
[64] Y.M. Deng, G.L. He, P. Kuppusamy, J.L. Zweier, Deconvolution algorithm based on automatic cutoff frequency selection for EPR imaging, Magnetic Resonance in Medicine 50 (2003) 444–448.
[65] Y. Liu, F.A. Villamena, J.L. Zweier, Highly stable dendritic trityl radicals as oxygen and pH probe, Chemical Communications (2008) 4336–4338.
[66] B. Driesshaert, N. Charlier, B. Gallez, J. Marchand-Brynaert, Synthesis of two persistent fluorinated tetrathiatriarylmethyl (TAM) radicals for biomedical EPR applications, Bioorganic & Medicinal Chemistry Letters 18 (2008) 4291–4293.
[67] I. Dhimitruka, A.A. Bobko, C.M. Hadad, J.L. Zweier, V.V. Khramtsov, Synthesis and characterization of amino derivatives of persistent trityl radicals as dual function pH and oxygen paramagnetic probes, Journal of the American Chemical Society 130 (2008) 10780–10787.
[68] S. Matsumoto, M.G. Espev, H. Utsumi, N. Devasahayam, K. Matsumoto, A. Matsumoto, H. Hirata, D.A. Wink, P. Kuppusamy, S. Subramanian, J.B. Mitchell, M.C. Krishna, Dynamic monitoring of localized tumor oxygenation changes using RF pulsed electron paramagnetic resonance in conscious mice, Magnetic Resonance in Medicine 59 (2008) 619–625.
[69] G. Ilangovan, A. Manivannan, H. Li, H. Yanagi, J.L. Zweier, P. Kuppusamy, A naphthalocyanine-based EPR spin probe for localized measurements of tissue oxygenation, Free Radical Biology and Medicine 32 (2002) 139–147.
[70] R.P. Pandian, N.L. Parinandi, G. Ilangovan, J.L. Zweier, P. Kuppusamy, Novel particulate spin probe for targeted determination of oxygen in cells and tissues, Free Radical Biology and Medicine 35 (2003) 1138–1148.
[71] S. Som, L.C. Potter, R. Ahmad, D.S. Vikram, P. Kuppusamy, EPR oximetry in the three spatial dimensions using sparse spin distribution, Journal of Magnetic Resonance 198 (2008) 210–217.
[72] D.S. Vikram, A. Bratasz, R. Ahmad, P. Kuppusamy, A comparative evaluation of EPR and OxyLite oximetry using a random sampling of $p(O_2)$ in a murine tumor, Radiation Research 168 (2007) 308–315.
[73] D.S. Vikram, R. Ahmad, R.P. Pandian, S. Petryakov, P. Kuppusamy, Evaluation of oxygen-responsive times of phthalocyanine-based crystalline paramagnetic spin probes for EPR oximetry, Journal of Magnetic Resonance 193 (2008) 127–132.